

石油学报

(石油加工)

第 27 卷 第 1 期 2011 年 2 月

目次

研究报告

- 催化裂化汽油馏分烯烃加氢反应动力学模型..... 石玉林 李大东 习远兵 董建伟(1)
- 减压蜡油加氢脱氮宏观反应动力学模型..... 张富平 胡志海 董建伟 李大东(5)
- 硅-铝催化剂酸中心形成及其结构* 贺振富 代振宇 龙军(11)
- 菲在不同加氢催化剂上的转化..... 李会峰 刘锋 刘泽龙 李明丰 聂红(20)
- Co 负载量对 Co/ γ -Al₂O₃ 催化剂 F-T 合成催化性能的影响.....
..... 罗熙 侯朝鹏 吴玉 夏国富 聂红(26)
- 不同来源渣油加氢反应性能的对比..... 孙昱东 杨朝合 山红红 赵辉 沈本贤(32)
- γ -Al₂O₃ 负载的 Mo 及 Ni-Mo 氮化物、碳化物的合成及其加氢脱氧性能
..... 张伟 张晔 赵亮富 魏伟(37)
- 硫酸亚铁/异丁醛/甲酸/过氧化氢体系 FCC 汽油的深度氧化脱硫
..... 林朋 郭伟 王成勇 吕效平(42)
- 负载氧化钴的碳纳米管催化剂催化氧化环己烷..... 新海波 原伟伟 郭志武(47)
- 氟改性的镁-铝复合氧化物催化酯交换反应制备生物柴油 吴功德 王晓丽 魏伟 孙子罕(54)
- FCC 沉降器粗旋风分离器的料腿泄气率 刘书贤 孙国刚 付烜 时铭显(62)
- 提升管加床层反应器提升管段下行颗粒的分布及其对流动的影响..... 王德武 卢春喜 严超宇(69)
- 表面活性剂界面吸附行为的分子动力学模拟..... 刘国宇 顾大明 丁伟 于涛 程杰成(77)
- NaCl 存在下 SDBS 与超高相对分子质量 AM-AA-AMPS 三元共聚物的相互作用
..... 孙焕泉 张玉玺 李振泉 曹绪龙 吴飞鹏(85)
- 柴油-甲醇-乳化剂三元组乳化液的制备及其理化特性 焦纬洲 刘有智 祁贵生 上官民(91)
- 用烃类族组成预测神华煤直接液化柴油的十六烷值..... 吴秀章 金环年 石玉林(95)
- 委内瑞拉原油中钒卟啉的分离和鉴定..... 高媛媛 沈本贤 刘纪昌(101)
- 辽河油田石脑油中有机氯化物的形态鉴定及脱除..... 樊秀菊 朱建华 宋海峰 武本成(107)
- 润滑油黏度可见/近红外光谱快速无损检测方法 蒋璐璐 张瑜 刘飞 谈黎虹 何勇(112)
- 苯磺酸钠表面活性剂在聚丙烯酰胺键合硅胶固定相上作用的热力学
..... 孙敏 李振泉 宋新旺 刘霞 蒋生祥(117)
- 萃取分离低浓度 DMF 含盐废水的液-液平衡 方静 李春利 王洪海 刘继东(123)

研究报道

- 以浏阳海泡石为原料原位合成 NaY 分子筛及其表征 韩勇 钱东 郑淑琴 黄石(130)
- 负载型多钒杂多酸催化剂在氧化脱硫反应中的应用..... 唐博合金 何文卿 李筱艺 徐吴瑕 徐菁利(134)
- 高温热处理对石油焦结构及气化活性的影响..... 刘鑫 张保申 周志杰 许建良 王辅臣(138)
- 茂金属催化的丙烯淤浆聚合模型: 聚丙烯相对分子质量分布 黄凯 谢瑞金 罗正鸿(144)
- 基于旋流的天然气超声速喷管分离特性..... 文闯 曹学文 张静 杨燕 张文敬(150)

信息

Ei 对中英文摘要的要求(10);《石油炼制与化工》征订启事(19);关于《石油学报(石油加工)》网上投稿的特别声明(61);《石油学报(石油加工)》征订启事(90);关于“全国第十六届润滑油技术交流暨三十周年纪念活动”征文通知(111);《China Petroleum Processing and Petrochemical Technology》征订启事(143)

* 封面文章

期刊基本参数: CN11-2129/TE*1985*b*A4*154*zh+en*P*¥15.00*1500*26*2011-2 本期责任编辑: 黄晓晖

ACTA PETROLEI SINICA

(PETROLEUM PROCESSING SECTION)

Vol. 27 No. 1 Feb. 2011

CONTENTS

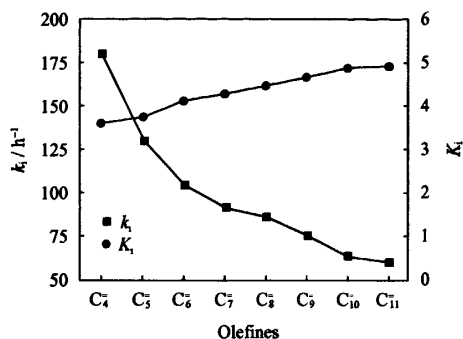
Research Articles

Acta Petrolei Sinica (Petroleum Processing Section), 2011, 27(1): 1-4 doi: 10.3969/j.issn.1001-8719.2011.01.001

Dynamic Models of the Olefin Hydrosaturation Reactions in FCCN

SHI Yulin LI Dadong XI Yuanbing DONG Jianwei

Hydrotreating reactions of olefin in FCC Naphtha (FCCN) and three reaction mechanisms for olefin hydrosaturation were studied. Plant pilot results showed that olefin reactions agreed with Langmuir-Hinshelwood mechanism, based on which, the dynamic models for hydrosaturation reactions of olefins with different carbon-number were set up.

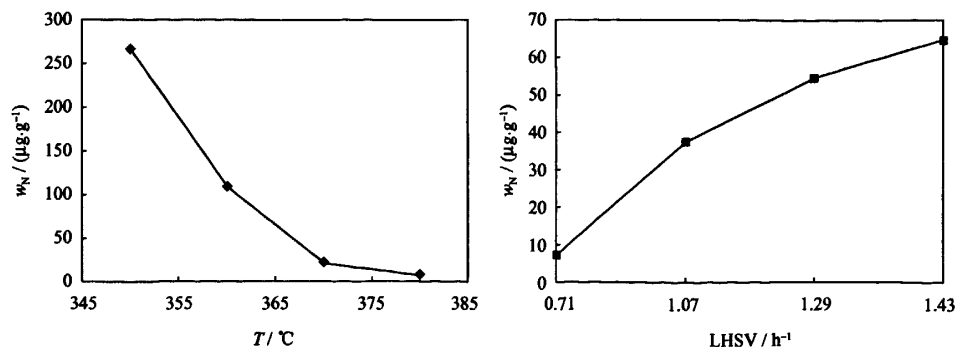


Acta Petrolei Sinica (Petroleum Processing Section), 2011, 27(1): 5-10 doi: 10.3969/j.issn.1001-8719.2011.01.002

Hydro-Denitrification Kinetics Macro Model for Vacuum Hydrowax

ZHANG Fuping HU Zhihai DONG Jianwei LI Dadong

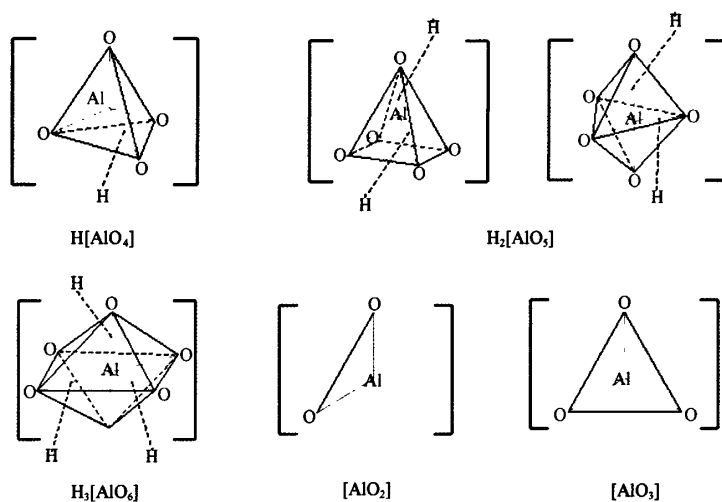
According to the characteristics of hydrotreating reactions, the effects of processing conditions on hydrodenitrification were examined. On the basis of a large number of HDN experimental data of VGO over RN-32 HT catalyst, the basic HDN reaction kinetic equation was suggested. Experimental data proved that this model was very successful.



Formation and Structural Characteristics of Acidic Centers of Silica-Alumina Catalyst

HE Zhenfu DAI Zhenyu LONG Jun

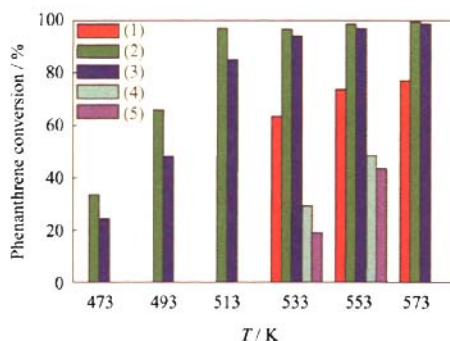
The catalytic activity of silica-alumina catalyst heavily depends on its acidic properties. The silica-alumina catalyst has three kinds of Brønsted acid centers and two kinds of Lewis acid centers. One 4-coordinated Brønsted acid center can provide one hydrogen proton. One 5-coordinated Brønsted acid center can provide two hydrogen protons. One 6-coordinated Brønsted acid center can provide three protons. The $[\text{AlO}_2]$ unit is a 2-coordination Lewis acid center, and the $[\text{AlO}_3]$ unit is a three-coordination Lewis acid center.



Hydrogenation of Phenanthrene Over Different Catalysts

LI Hui Feng LIU Feng LIU Zelong LI Mingfeng NIE Hong

Compared with $\text{CoMo}/\text{Al}_2\text{O}_3$, $\text{NiMo}/\text{Al}_2\text{O}_3$ and $\text{NiW}/\text{Al}_2\text{O}_3$ exhibit higher activity in phenanthrene hydrogenation moreover, $\text{NiMo}/\text{Al}_2\text{O}_3$ shows better hydrogenation activity than $\text{NiW}/\text{Al}_2\text{O}_3$ at relatively lower reaction temperatures, which is mainly due to the difference of the promoting effect of Ni and Co on Mo (W).

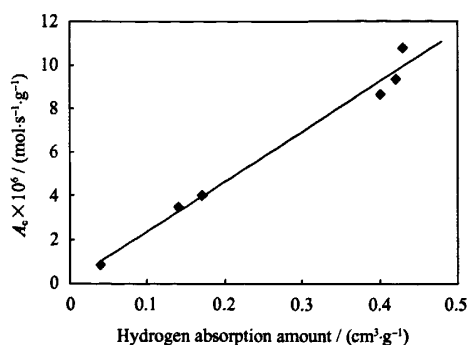


(1) $\text{CoMo}/\text{Al}_2\text{O}_3$; (2) $\text{NiMo}/\text{Al}_2\text{O}_3$; (3) $\text{NiW}/\text{Al}_2\text{O}_3$;
(4) $\text{Mo}/\text{Al}_2\text{O}_3$; (5) $\text{W}/\text{Al}_2\text{O}_3$

Influence of Cobalt Loading on Catalytic Performance of Co/ γ -Al₂O₃ Catalysts in Fischer-Tropsch Synthesis

LUO Xi HOU Chaopeng WU Yu XIA Guofu NIE Hong

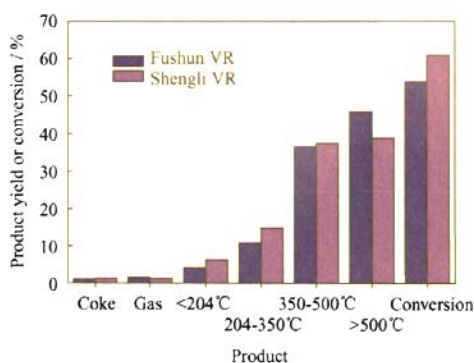
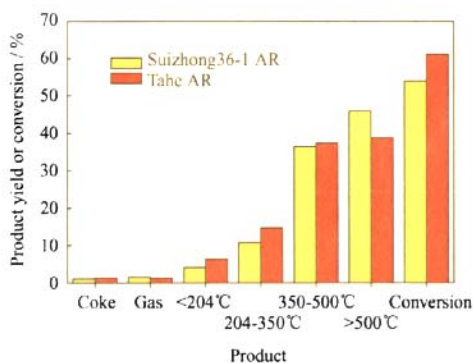
A series of Co/ γ -Al₂O₃ with different Co loadings were prepared. The results showed that both the catalytic activity and the reduction extent of Co/ γ -Al₂O₃ catalyst first increased then decreased with the increase of Co loading. There was a linear relationship between the catalytic activity and hydrogen absorption amount of H₂ for Co/ γ -Al₂O₃ catalyst.



Hydrotreating Reaction Performance of Different Residua

SUN Yudong YANG Chaohu SHAN Honghong ZHAO Hui SHEN Benxian

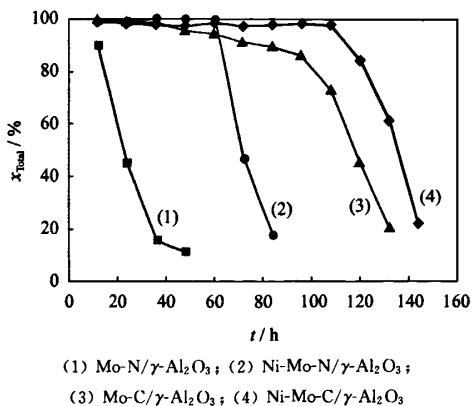
Four kinds of residue were hydrotreated in autoclave. It is demonstrated that the poor residua (high asphaltene content) have high conversion, high light oil yield, low residue yield and slightly high coke yield. Asphaltene is mainly hydrocracked to the compounds of smaller molecule in residue hydrotreating when asphaltene content is high in feedstock.



Synthesis and Hydrodeoxygenation Activity of Mo, Ni-Mo Nitride and Carbide Supported on γ -Al₂O₃

ZHANG Wei ZHANG Ye ZHAO Liangfu WEI Wei

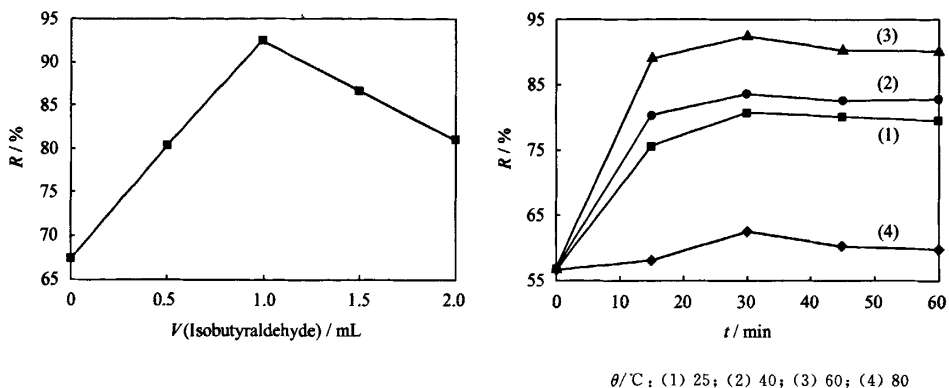
Mo and Ni-Mo nitride and carbide catalysts were synthesized by means of temperature-programmed reaction. The hydrodeoxygenation(HDO) performance of the catalysts was investigated by using ethyl benzoate as a model compound. The results indicated that both the nitride and carbide catalysts exhibited high activities for HDO of ethyl benzoate, but carbide was superior to nitride in stability.



Deep Oxidation Desulfurization of FCC Gasoline With Ferrous Sulfate/Isobutyraldehyde/Formic Acid/Hydrogen Peroxide System

LIN Peng GUO Wei WANG Chengyong LÜ Xiaoping

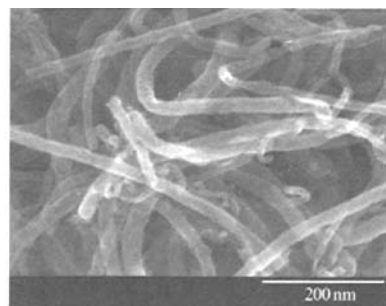
The oxidation desulfurization of FCC gasoline by using the system of ferrous ion / isobutyraldehyde / formic acid / hydrogen peroxide was studied. The results showed that this system greatly enhanced the oxidation desulfurization. Under particular conditions, the desulfurization rate of FCC gasoline can reach 92.39% in 30 min.



Catalytic Oxidation Reaction of Cyclohexane on Co₃O₄ Supported Carbon Nanotube Catalysts

JIN Haibo YUAN Weiwei GUO Zhiwu

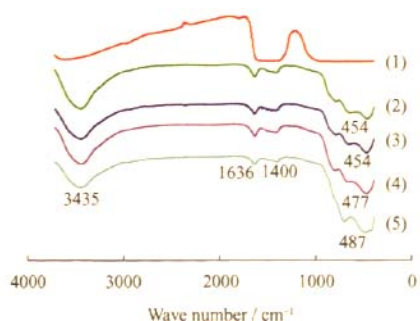
Carbon nanotubes supported Co₃O₄ catalysts were prepared by using the method of impregnation-deposition. The effects of cobalt nitrate concentration, reaction time, system temperature, amounts of catalyst and initiator on cyclohexane oxidation reaction were investigated. Under the optimum oxidation reaction conditions, the conversion of cyclohexane oxidation was 14.2%, and the total selectivity of cyclohexanol, clohexanone and cyclohexyl hydroperoxide was 90.2%.



Preparation of Biodiesel by Transesterification Over Fluorine-Modified Mg-Al Mixed Oxides

WU Gongde WANG Xiaoli WEI Wei SUN Yuhan

Fluorine-modified Mg-Al mixed oxides were prepared at different calcination temperatures. In the preparation of biodiesel by transesterification of soybean oil and methanol, the obtained samples exhibited much better catalytic performance than the pure Mg-Al mixed oxides, which could be ascribed to the appearance of MgF₂ species.

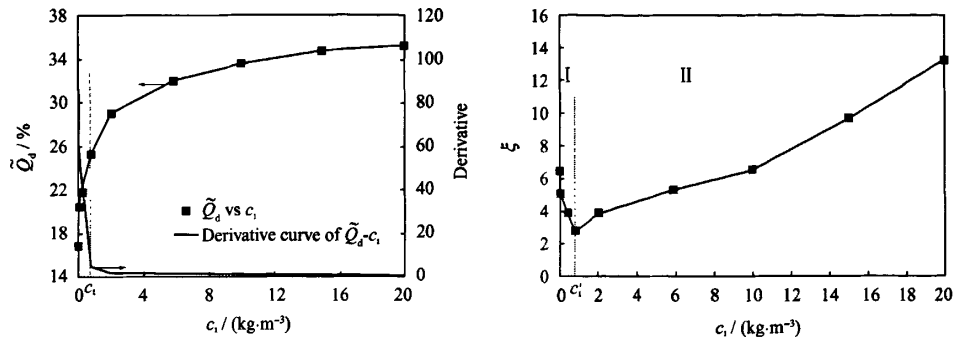


(1) Mg₃(Al)O-450; (2) F/Mg₃(Al)O-400; (3) F/Mg₃(Al)O-450; (4) F/Mg₃(Al)O-600; (5) F/Mg₃(Al)O-800

Gas-Leakage Ratio of Rough-Cut Cyclone Dipleg in FCC Disengager

LIU Shuxian SUN Guogang FU Xuan SHI Mingxian

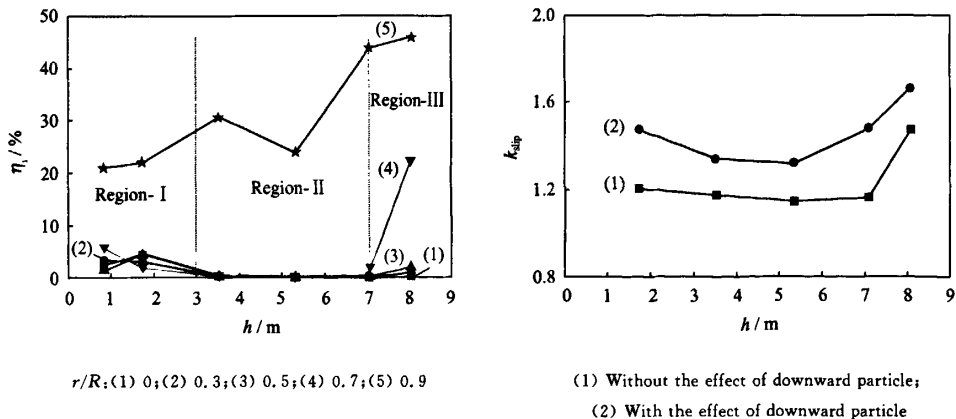
Gas-leakage ratio of rough-cut cyclone increased with the solid concentration going from steep to mild, with turning point around concentration (c_i) of 0.8 kg/m³, in correspondence with the concentration-pressure drop relation, which was caused by the wrapping function of agglomerated particles and the reduction on gas flow cross section by solid layer onto the wall.



Downward Particle Distribution and Its Effects on Particle Flow in the Riser Section of Riser-Fluidized Bed Reactor

WANG Dewu LU Chunxi YAN Chaoyu

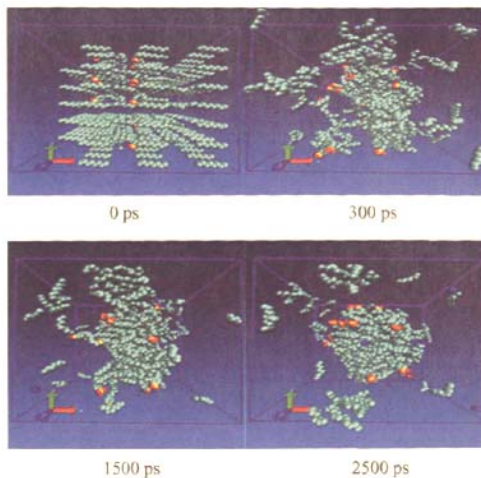
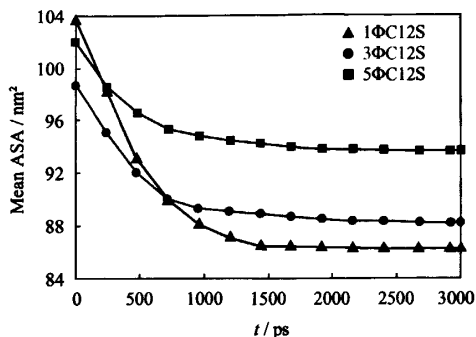
The downward particles in the outlet restriction region of the riser distributed mainly in the region close to wall with the non-dimensional radial position $r/R \geq 0.70$. The downward particle fraction was mainly affected by outlet restriction resistance, which increased with an increase of outlet restriction resistance.



Molecular Dynamics Simulation of Anionic Surfactant Aggregation at the Interface

LIU Guoyu GU Daming DING Wei YU Tao CHENG Jiecheng

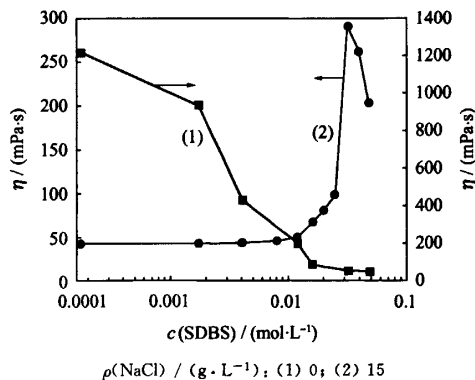
The separation process of oil-water and the properties of sodium dodecyl benzene sulfonate adsorbed at the water-oil interface were investigated by using molecular dynamics (MD) simulations, considering the variation of molecular structure and the concentration of sodium dodecyl benzene sulfonate in oil-water system.



Interactions Between AM-AA-AMPS Copolymer With Super-High Molecular Mass and SDBS in Aqueous Solution in the Presence of Sodium Chloride

SUN Huanquan ZHANG Yuxi LI Zhenquan CAO Xulong WU Feipeng

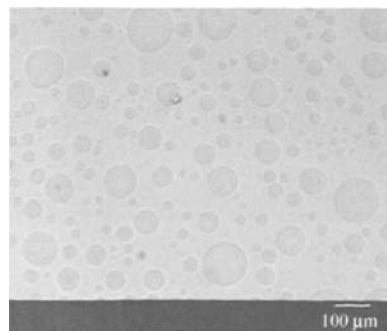
In the presence of sodium chloride (NaCl), acrylamide (AM)/sodium acrylate(AA)/2-acrylamido-2-methyl-1-propanesulphonate sodium (AMPS) copolymer and sodium dodecylbenzene sulphonate (SDBS) could form a complex of copolymer-SDBS with cross-linked networks in aqueous solution, which exhibited special viscosity behavior. The copolymer-SDBS complex was sensitive to temperature, with the temperature rising, the complex gradually dissolved in aqueous solution.



Physicochemical Properties of the Emulsions Made by Diesel, Methanol and Emulsifier

JIAO Weizhou LIU Youzhi QI Guisheng SHANGGUAN Min

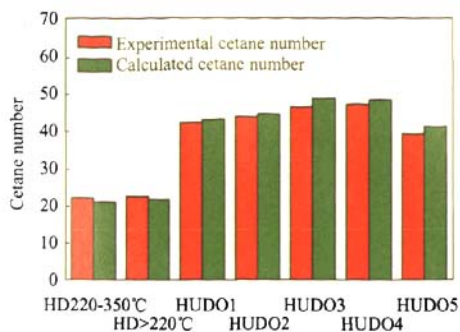
By using the advanced video-microscopy technique, it is found that the droplet size of disperse phase in emulsified fuel decreased with the augment of the emulsifier amount, and almost contrary to the methanol content. The mean diameter of the disperse phase can be adjusted in the range of 12–50 μm through the control of operation conditions.



Cetane Number Prediction of Shenhua Direct Coal Liquefaction Diesel Oil With Hydrocarbon Group Composition

WU Xiuzhang JIN Huannian SHI Yulin

A correlation equation between cetane number of the direct coal liquefaction diesel oil and hydrocarbon group composition was established, which could well predict its cetane number, with the absolute error of below 3 and the standard deviation of 1.47.

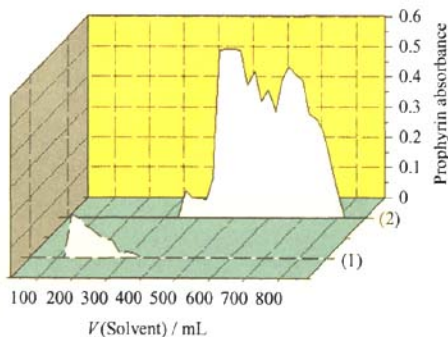
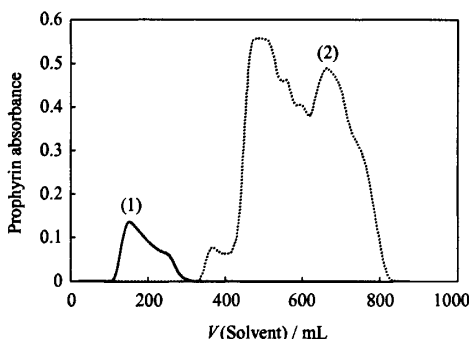


HD—Hydrogenation product, HUDO—Hydro-upgrading diesel oil

Isolation and Characterization of Vanadium Porphyrins in Venezuela Crude Oil

GAO Yuanyuan SHEN Benxian LIU Jichang

The various types of porphyrins could be separated efficiently by using silica gel column. The contents of ETIO and DPEP homologues in vanadium porphyrins of Venezuela crude oil are 80.7% and 19.3%, respectively. Furthermore, the C₂₈-ETIO and the C₃₁-DPEP show the largest abundance.

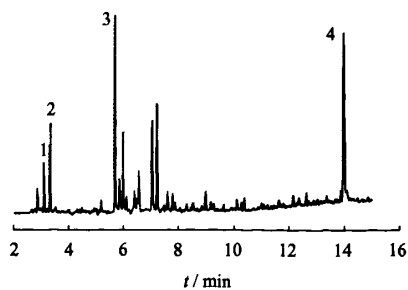


(1) Nickel porphyrin; (2) Vanadium porphyrin

Pattern Identification and Removal of Organic Chlorine in Naphtha From Liaohe Oilfield

FAN Xiuju ZHU Jianhua SONG Haifeng WU Bencheng

Organochlorines in naphtha were identified and quantified by gas chromatography with ECD. The results showed that the organic chlorines in naphtha were existed mainly in the forms of chloroform, carbon tetrachloride, tetrachloroethane and 1,2-dichlorobenzene, and their mass concentration were 0.16, 0.02, 3.32 and 4.52 mg/L, respectively.

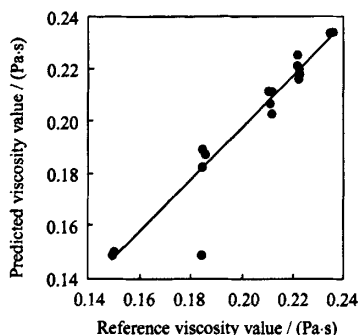


1—Chloroform; 2—Carbon tetrachloride; 3—Tetrachloroethane; 4—1,2-Dichlorobenzene

Fast and Nondestructive Detection for Viscosity of Lubricating Oil Using Visible/Near Infrared Spectroscopy

JIANG Lulu ZHANG Yu LIU Fei TAN Lihong HE Yong

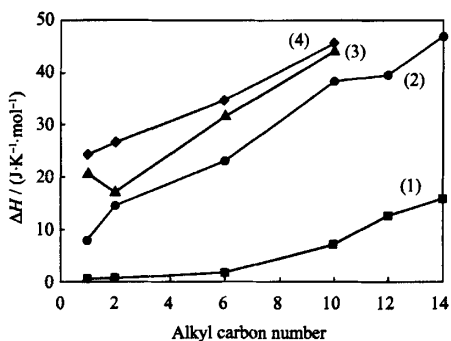
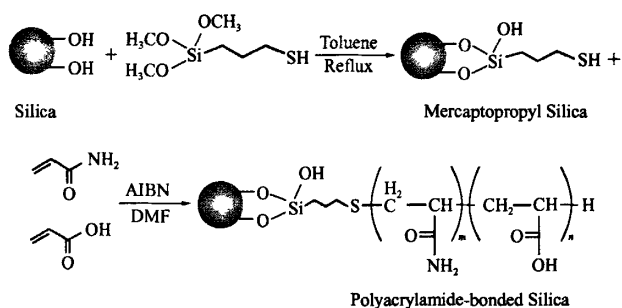
Visible/near infrared spectroscopy was successfully used for the fast and nondestructive determination of viscosity of lubricating oil. The optimal calibration model was achieved by back propagation neural network (BPNN) with the principal components extracted by principal component analysis (PCA), and the correlation coefficient (r) of validation set was 0.971.



Thermodynamics of Sodium *p*-*n*-Alkylbenzene Sulfonates Surfactants on Partial Hydrolytic Polyacrylamide-Bonded Silica Stationary Phase

SUN Min LI Zhenquan SONG Xinwang LIU Xia JIANG Shengxiang

The partial hydrolytic polyacrylamide-bonded silica was prepared and used as a new stationary phase. The thermodynamics of the interaction between sodium *p*-*n*-alkylbenzene sulfonates and partial hydrolytic polyacrylamide was investigated by high performance liquid chromatography. The quantitative analysis of both their interactions and the conformational change of sodium *p*-*n*-alkylbenzene sulfonates were obtained.

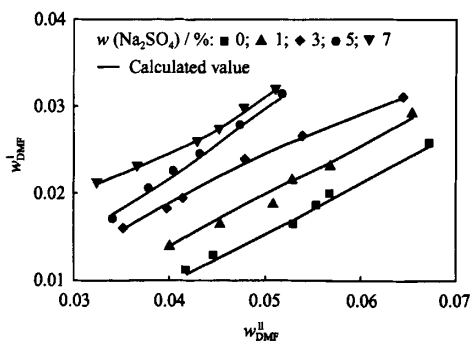


Mobile phase: (1) $V(\text{Methanol})/V(\text{H}_2\text{O}) = 10/90$; (2) H_2O ; (3) Simulated formation water with salinity of 5700; (4) Simulated formation water with salinity of 8800

Liquid-Liquid Equilibrium for Saliniferous Wastewater Containing Low Concentration of DMF in Extraction Process

FANG Jing LI Chunli WANG Honghai LIU Jidong

Liquid-liquid equilibrium data for the saliniferous system of DMF-water-chloroform with different mass fractions of Na_2SO_4 were determined under atmospheric pressure and 293.15 K. The experimental data showed that the partition coefficient of DMF in DMF-water-chloroform system increased with the increase of Na_2SO_4 mass fraction.

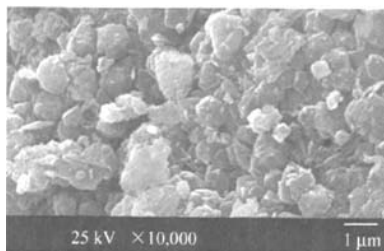


Acta Petrolei Sinica (Petroleum Processing Section), 2011, 27(1): 130-133 doi: 10.3969/j.issn.1001-8719.2011.01.022

In-Situ Synthesis and Characterization of NaY Zeolite From Liuyang Sepiolite

HAN Yong QIAN Dong ZHENG Shuqin HUANG Shi

NaY zeolite with a high surface area, large pore volume and high $n(\text{SiO}_2)/n(\text{Al}_2\text{O}_3)$ ratio in the framework was successfully synthesized by an *in-situ* technique under hydrothermal conditions with calcined sepiolite and metakaolin as the raw materials.

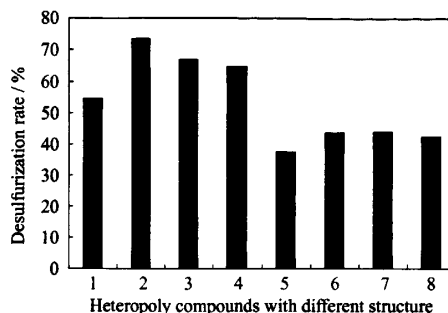


Acta Petrolei Sinica (Petroleum Processing Section), 2011, 27(1): 134-137 doi: 10.3969/j.issn.1001-8719.2011.01.023

Application of Vanadium Substituted Heteropoly Acid Catalyst in Oxidative Desulfurization Reaction

TANG Bohejin HE Wenqing LI Xiaoyi XU Wuxia XU Jingli

Dawson-type vanadium substituted heteropoly acid of $\text{H}_{12}\text{P}_2\text{Mo}_{12}\text{V}_6\text{O}_{62}$, $\text{H}_{14}\text{P}_2\text{Mo}_{10}\text{V}_8\text{O}_{62}$, $\text{H}_{15}\text{P}_3\text{Mo}_{18}\text{V}_6\text{O}_{84}$ and $\text{H}_{12}\text{P}_3\text{Mo}_{18}\text{V}_7\text{O}_{85}$ were synthesized. The oxidative desulfurization performances of the catalysts with these heteropoly acids as active components were investigated by using dibenzothiophene (DBT) as model compound. The result showed that $\text{H}_{12}\text{P}_3\text{Mo}_{18}\text{V}_7\text{O}_{85}/\text{C}$ demonstrated excellent catalytic performance in the oxidative desulfurization reaction of DBT.



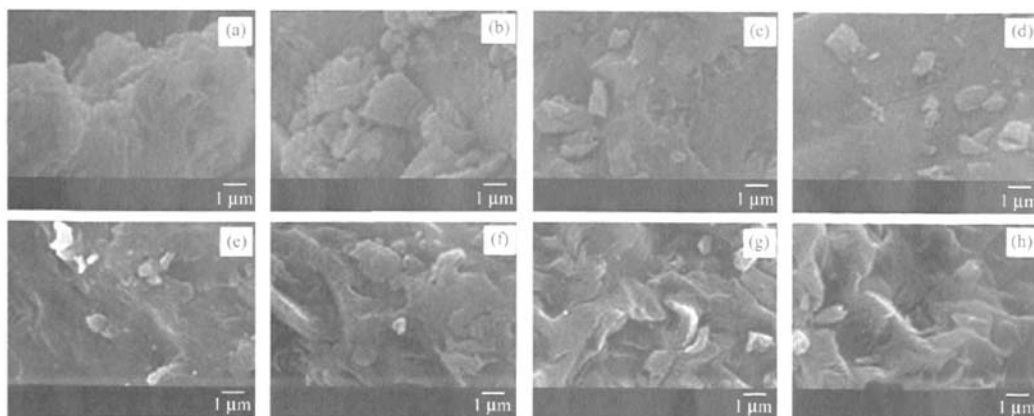
Heteropoly compounds with different structure
 1— $\text{H}_{12}\text{P}_2\text{Mo}_{12}\text{V}_6\text{O}_{62}/\text{C}$; 2— $\text{H}_{12}\text{P}_3\text{Mo}_{18}\text{V}_7\text{O}_{85}/\text{C}$;
 3— $\text{H}_{15}\text{P}_3\text{Mo}_{18}\text{V}_6\text{O}_{84}/\text{C}$; 4— $\text{H}_{14}\text{P}_2\text{Mo}_{10}\text{V}_8\text{O}_{62}/\text{C}$;
 5— $\text{H}_{12}\text{P}_2\text{Mo}_{12}\text{V}_6\text{O}_{62}/\text{SiO}_2$; 6— $\text{H}_{12}\text{P}_3\text{Mo}_{18}\text{V}_7\text{O}_{85}/\text{SiO}_2$;
 7— $\text{H}_{14}\text{P}_2\text{Mo}_{10}\text{V}_8\text{O}_{62}/\text{SiO}_2$; 8— $\text{H}_{15}\text{P}_3\text{Mo}_{18}\text{V}_6\text{O}_{84}/\text{SiO}_2$

Acta Petrolei Sinica (Petroleum Processing Section), 2011, 27(1): 138-143 doi: 10.3969/j.issn.1001-8719.2011.01.024

Structure Changes and Gasification Activity of Petroleum Coke After Heat Treatment

LIU Xin ZHANG Baoshen ZHOU Zhijie XU Jianliang WANG Fuchen

The influences of high temperature treatment on the structure, the degree of graphitization and the gasification reactivity of petroleum coke were investigated. The results showed that the high temperature treatment could increase the degree of graphitization and inhibit the gasification reactivity of petroleum coke.

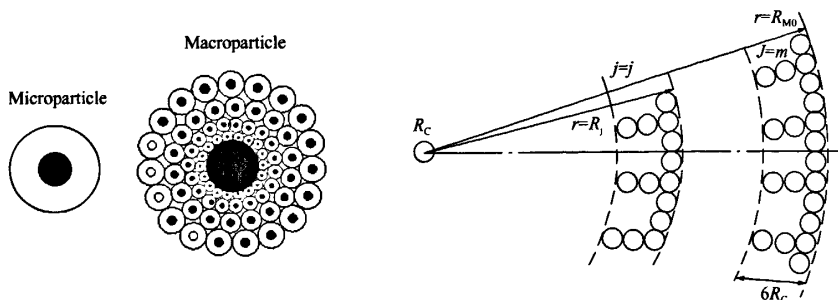


(a),(b),(c),(d) P1; (e),(f),(g),(h) P2
 (a),(e) Untreated; T_h/K : (b) 1173; (c) 1473; (d) 1673; (f) 1173; (g) 1473; (h) 1673

Model of the Slurry Propylene Polymerization Catalyzed by Metallocene Catalysts; Relative Molecular Mass Distribution of Polypropylene

HUANG Kai XIE Ruijin LUO Zhenghong

A particle growth model was suggested to simulate the relative molecular mass distribution (MMD) of polypropylene made via slurry polymerization catalyzed by a silica-supported metallocene catalyst. The simulated results showed that the mass transfer resistance can greatly influence the polymerization during its early stage, which can explain why the MMD broadened.



Separation Characteristics of Supersonic Swirling Flow Nozzle for Natural Gas

WEN Chuang CAO Xuewen ZHANG Jing YANG Yan ZHANG Wenjing

The channel between the wall and the central body formed a new Laval nozzle, at the entrance of which some twisted vanes were located to generate swirling flow. The effects of the convergent, throat and divergent sections on swirling separation performance were calculated with the RNG $k-\epsilon$ turbulence model.

